# ICES REPORT 18-14

## August 2018

# Augmented lagrangian for treatment of hanging nodes in hexahedral meshes

**by**

Saumik Dana and Mary F. Wheeler


**The Institute for Computational Engineering and Sciences**
The University of Texas at Austin
Austin, Texas 78712

*Reference: Saumik Dana and Mary F. Wheeler, "Augmented lagrangian for treatment of hanging nodes in hexahedral meshes," ICES REPORT 18-14, The Institute for Computational Engineering and Sciences, The University of Texas at Austin, August 2018.*

# Augmented lagrangian for treatment of hanging nodes in hexahedral meshes

Saumik Dana[a], Mary. F. Wheeler[a]

[a]*Center for Subsurface Modeling, Institute for Computational Engineering and Sciences, The University of Texas at Austin, TX 78712*

**Abstract**

The surge of activity in the resolution of fine scale features in the field of earth sciences over the past decade necessitates the development of robust yet simple algorithms that can tackle the various drawbacks of in silico models developed hitherto. One such drawback is that of the restrictive computational cost of finite element method in rendering resolutions to the fine scale features, while at the same time keeping the domain being modeled sufficiently large. We propose the use of the augmented lagrangian method commonly used in the treatment of hanging nodes in contact mechanics in tackling the drawback. An interface is introduced in a typical finite element mesh across which an aggressive coarsening of the finite elements is possible. The method is based upon minimizing an augmented potential energy which factors in the constraint that exists at the hanging nodes on that interface. This allows for a significant reduction in the number of finite elements comprising the mesh with concomitant reduction in the computational expense.

## 1. Introduction

The quantum of work devoted to modeling of fine scale features in the subsurface in the recent decade has spawned a need for simple yet powerful algorithms to simulate the same in silico with low computational cost. The main barrier to these simulations lies in the restrictively fine mesh that needs to be invoked to resolve the finer features of the corresponding physics, while at the same time keeping the domain under consideration sufficiently large. The most logical approach to this problem is to allow for a fine mesh to

*Email addresses:* saumik@utexas.edu (Saumik Dana), mfw@ices.utexas.edu (Mary. F. Wheeler)

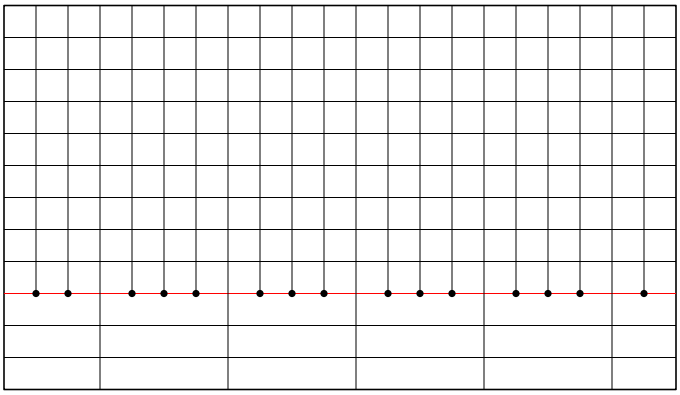

Figure 1: A 2D depiction of the problem of hanging nodes for the sake of convenience. The hanging nodes are represented by dots. The interface is represented by a red line

exist in the regions which need a fine mesh, and a coarse mesh to exist in regions which do not need a fine mesh. The authors have in the past developed a method to simulate subsurface flow on a fine mesh and subsurface mechanics on a coarse mesh while allowing for the coupling between the physics of flow and mechanics via a staggered solution algorithm (Dana et al. [2]). The aforementioned work, though, is restrictive in the sense that the mesh for the mechanics domain needs to be uniformly coarser than the mesh for the flow domain. This makes the algorithm infeasible for problems involving fine scale features for the mechanics. With that in mind, in this work, we propose an addendum to the aforementioned algorithm. We invoke the concept of hanging nodes in finite elements. It essentially means that there is an interface in the mechanics mesh across which an aggressive refinement is possible, thus allowing for fine elements on one side of the interface and coarser elements on the other side of the interface. A 2D depiction of the idea is given in Figure 1 and a 3D depiction is given in Figure 2.

### *1.1. Summary of the various formulations for treatment of hanging nodes developed hitherto*

The concept of hanging nodes itself is not new, and has been given its due diligence as far back as in the 1980s, 1990s and early 2000s (see the works of Felippa [4], Powell [10], Hallquist et al. [5], Simo et al. [13], Wriggers and Simo [15], Parisch [9], Papadopoulos and Taylor [7], Papadopoulos and Taylor [8], McDevitt and Laursen [6], El-Abbasi and Bathe [3], Becker et al. [1], Puso and Laursen [11], Puso and Laursen [12], Wriggers [14] and Wriggers

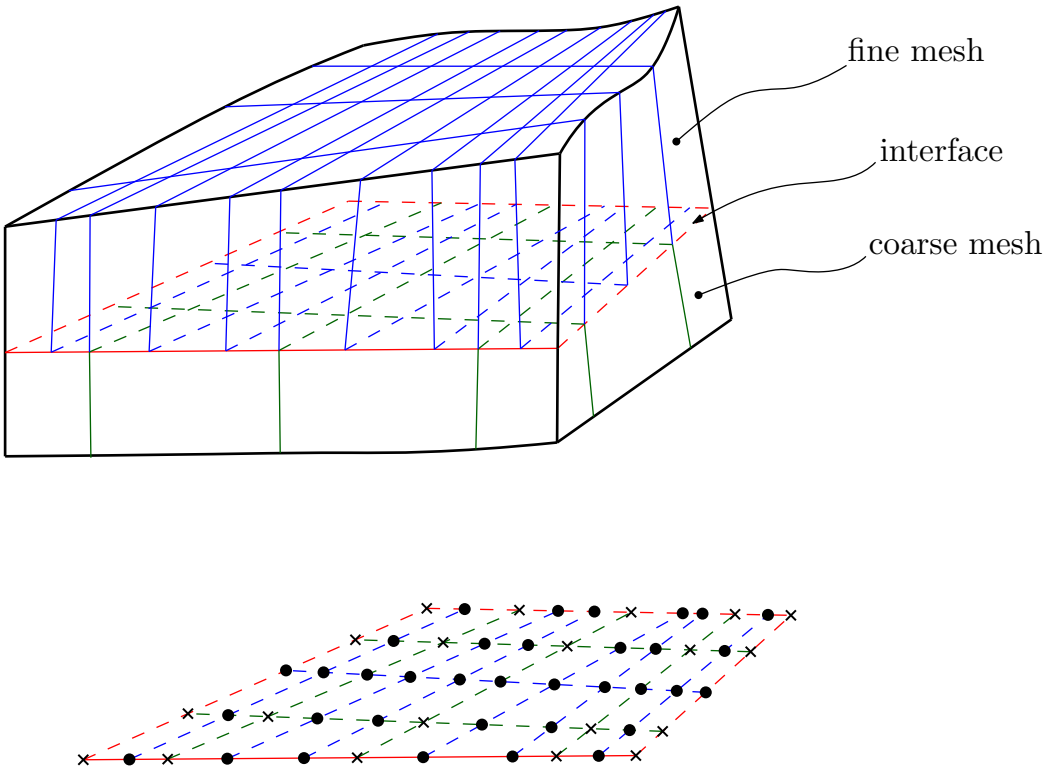


Figure 2: A 3D depiction of the problem of hanging nodes. The hanging nodes are represented by dots. The boundary of the interface is represented by a red dashed line. Crosses represent the nodes that are common to both the fine and coarse mesh

and Zavarise [16]). The problem is looked upon as optimization of a functional with a constraint which dictates the geometry of the interface of the hanging nodes. Representing $\mathscr{C}(\mathbf{u})$ as the potential energy functional of a system with $\mathbf{u}$ respresenting the displacement field, the optimization problem statement is simply put forth as: Minimize $\mathscr{C}(\mathbf{u})$ subject to a constraint $\mathbf{g}(\mathbf{u}) = \mathbf{0}$. The *penalty formulation* penalizes the non-satisfaction of the constraint by augmenting the energy functional to be minimized as follows

$$\tilde{\mathscr{C}}(\mathbf{u}) = \mathscr{C}(\mathbf{u}) + \frac{\epsilon}{2}\mathbf{g}(\mathbf{u}) \cdot \mathbf{g}(\mathbf{u})$$

where $\epsilon$ is a large penalty parameter. A large enough penalty parameter closes the gap between the solution obtained through the penalty formulation and the original minimization problem solution. On the other hand, a large penalty parameter leads to highly ill-conditioned stiffness matrix in the eventual system of equations obtained at the discrete level. As a result, the choice of penalty parameter is a compromise between solution ac-

curacy and solution stability. The *lagrangian formulation*, on the other hand, enforces the constraint by introducing a lagrange multiplier term to the energy functional to be minimized as follows

$$\tilde{\mathscr{C}}(\mathbf{u}, \boldsymbol{\lambda}) = \mathscr{C}(\mathbf{u}) + \boldsymbol{\lambda} \cdot \mathbf{g}(\mathbf{u})$$

where $\boldsymbol{\lambda}$ is the force conjugate to the constraint $\mathbf{g}(\mathbf{u}) = 0$, and is refered to as the lagrange multiplier. Although this method allows for the exact satisfaction of the constraint, the increase in number of degrees of freedom of the original system by the number of lagrange multipliers makes the augmentation computationally expensive. The *perturbed Lagrangian formulation* circumvents this problem by introducing the following functional to be minimized

$$\tilde{\mathscr{C}}(\mathbf{u}, \boldsymbol{\lambda}) \equiv \mathscr{C}(\mathbf{u}) + \boldsymbol{\lambda} \cdot \mathbf{g}(\mathbf{u}) - \frac{1}{2\epsilon} \boldsymbol{\lambda} \cdot \boldsymbol{\lambda}$$

with the constraint

$$\mathbf{g}(\mathbf{u}) - \frac{\boldsymbol{\lambda}}{\epsilon} = \mathbf{0}$$

where $\epsilon$ is the penalty parameter. This allows for the lagrange multiplier to be posed in terms of the constraint thus negating the need to solve for the multiplier as an additional degree of freedom. This method, though, suffers from the same problem that the original penalty method suffers from, i.e. a careful compromise between accuracy and stability must be made in the choice of the penalty parameter. The *augmented Lagrangian formulation* circumvents this issue by introducing the following functional to be minimized

$$\tilde{\mathscr{C}}(\mathbf{u}, \boldsymbol{\lambda}^k) \equiv \mathscr{C}(\mathbf{u}) + \boldsymbol{\lambda}^k \cdot \mathbf{g}(\mathbf{u}) + \frac{\epsilon}{2} \mathbf{g}(\mathbf{u}) \cdot \mathbf{g}(\mathbf{u})$$

with the constraint

$$\boldsymbol{\lambda}^{k+1} - \boldsymbol{\lambda}^k = \epsilon \mathbf{g}(\mathbf{u})$$

where $\boldsymbol{\lambda}^k$ is the lagrange multiplier evaluated at the $k^{th}$ iteration. As is evident from the formulation, the lagrange multiplier is evaluated iteratively till it reaches an asymptotic value. The lagrange multiplier, is not an additional degree of freedom, and hence the

system size does not increase as compared to the original minimization problem. The biggest advantage of this method is that the solution stability is not a function of the penalty parameter, and furthermore the lagrange multiplier iterative process reaches the true asymptotic value regardless of the value of the penalty parameter.

## 2. The functional to be minimized

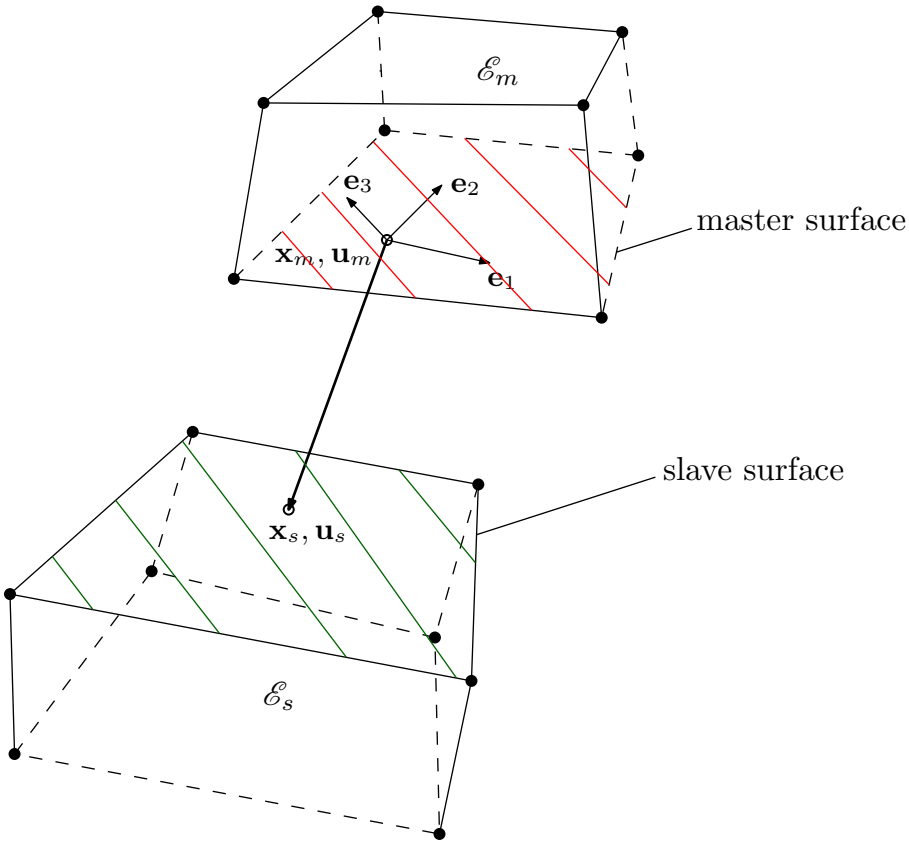


Figure 3: The interface containing hanging nodes is treated as a union of the coinciding faces of the finite elements on either side of the interface. One of the coinciding faces is refered to as the master surface while the other is refered to as the slave surface

From the geometrical standpoint, the interface is treated as a union of coinciding faces of the general hexahedral finite elements sharing the hanging nodes as shown in Figure 3. One of the faces is refered to as the *slave surface* while the other face is refered to as the *master surface*. Let us refer to elements containing the slave surfaces as *slave elements* and elements containing the master surfaces as *master elements*. Let $\mathbf{x}_s$ represent a generic point on the

surface of slave element $\mathscr{E}_s$ containing the slave surface and let $\mathbf{x}_m$ represent the *orthogonal projection* of $\mathbf{x}_s$ onto the surface of master element $\mathscr{E}_m$ containing the master surface. Let $\mathbf{u}_s$ and $\mathbf{u}_m$ represent the displacement field evaluated at $\mathbf{x}_s$ and $\mathbf{x}_m$ respectively. Let $\mathscr{C}^s$ and $\mathscr{C}^m$ be the strain energies of $\mathscr{E}_s$ and $\mathscr{E}_m$ respectively. Then the augmented functional to be minimized is

$$\tilde{\mathscr{C}} \equiv \overbrace{\mathscr{C}^s + \mathscr{C}^m}^{①} + \overbrace{\int_{\Gamma_c} \boldsymbol{\lambda} \cdot \mathbf{g}\, dA}^{②} + \overbrace{\frac{1}{2}\int_{\Gamma_c} \epsilon \mathbf{g} \cdot \mathbf{g}\, dA}^{③}$$

where $\mathbf{g} \equiv \mathbf{u}_s - \mathbf{u}_m$ is the refered to as the *penetration function*, $\boldsymbol{\lambda} \equiv \frac{1}{2}(\mathbf{t}^s + \mathbf{t}^m)$ is the force conjugate to the constraint $\mathbf{g} = \mathbf{0}$; introduced in a mean sense, and $\mathbf{t}^s$ and $\mathbf{t}^m$ are force conjugates to $\mathbf{g}$ at $\mathbf{x}_s$ and $\mathbf{x}_m$ respectively. The term ① is the total strain energy of $\mathscr{E}_s$ and $\mathscr{E}_m$, the term ② is the lagrange multiplier term and the term ③ is the penalty term. The term ② enforces the constraint $\mathbf{g} = \mathbf{0}$ via lagrange multipliers, and the term ③ penalizes any deviation from the constraint $\mathbf{g} = \mathbf{0}$. The integrals are evaluated with respect to one of the surfaces (in this case surface of $\mathscr{E}_s$ or the slave surface).

### *2.1. Orthogonal projections*

Let $\mathbf{X}_{m_i}$, $i = 1, .., 8$ and $\mathbf{X}_{s_j}$, $j = 1, .., 8$ be the coordinates of the finite element nodes of $\mathscr{E}_s$ and $\mathscr{E}_m$ respectively. Let $(\xi, \eta, \mu)$ represent the spatial field in reference element $\hat{\mathscr{E}}$ and let $N_i(\xi, \eta, \mu)$, $i = 1, .., 8$ represent the shape functions. Then we have

$$\left\{ \begin{array}{c} \mathbf{x}_m = \sum_{i=1}^{8} N_i|_{(\xi_m, \eta_m, \mu_m)} \mathbf{X}_{m_i} \\ \mathbf{x}_s = \sum_{i=1}^{8} N_i|_{(\xi_m, \eta_m, \mu_m)} \mathbf{X}_{s_i} \end{array} \right\} \tag{2.1}$$

where $(\xi_m, \eta_m, \mu_m)$ and $(\xi_s, \eta_s, \mu_s)$ are the coordinates of $\mathbf{x}_m$ and $\mathbf{x}_s$ respectively mapped onto the reference element $\hat{\mathscr{E}}$. It is critical to note that $(\xi_s, \eta_s, \mu_s)$ is known while $(\xi_m, \eta_m, \mu_m)$ is to be determined. The components $\mathbf{e}_1$, $\mathbf{e}_2$ and $\mathbf{e}_3$ of the tangent at $\mathbf{x}_m$ with respect to the local axis of master surface are computed as

$$\left\{ \begin{array}{l} \mathbf{e}_1 = \sum_{i=1}^{8} \frac{\partial N_i}{\partial \xi}|_{(\xi_m, \eta_m, \mu_m)} \mathbf{X}_{m_i} \\ \mathbf{e}_2 = \sum_{i=1}^{8} \frac{\partial N_i}{\partial \eta}|_{(\xi_m, \eta_m, \mu_m)} \mathbf{X}_{m_i} \\ \mathbf{e}_3 = \sum_{i=1}^{8} \frac{\partial N_i}{\partial \mu}|_{(\xi_m, \eta_m, \mu_m)} \mathbf{X}_{m_i} \end{array} \right\} \tag{2.2}$$

$\mathbf{x}_m$ is the orthogonal projection onto the master surface of $\mathbf{x}_s$ on the slave surface. The orthogonality condition is satisfied by

$$\left\{ \begin{array}{l} \mathbf{e}_1 \cdot (\mathbf{x}_s - \mathbf{x}_m) = 0 \\ \mathbf{e}_2 \cdot (\mathbf{x}_s - \mathbf{x}_m) = 0 \\ \mathbf{e}_3 \cdot (\mathbf{x}_s - \mathbf{x}_m) = 0 \end{array} \right\} \tag{2.3}$$

Substituting (2.1) and (2.2) in (2.3), we get

$$\left\{ \begin{array}{l} \sum_{j=1}^{8} \frac{\partial N_j}{\partial \xi}|_{(\xi_m,\eta_m,\mu_m)} \mathbf{X}_{m_j} \cdot \left( \mathbf{x}_s - \sum_{k=1}^{8} N_k|_{(\xi_m,\eta_m,\mu_m)} \mathbf{X}_{m_k} \right) \equiv f_1(\xi_m, \eta_m, \mu_m) = 0 \\ \sum_{j=1}^{8} \frac{\partial N_j}{\partial \eta}|_{(\xi_m,\eta_m,\mu_m)} \mathbf{X}_{m_j} \cdot \left( \mathbf{x}_s - \sum_{k=1}^{8} N_k|_{(\xi_m,\eta_m,\mu_m)} \cdot \mathbf{X}_{m_k} \right) \equiv f_2(\xi_m, \eta_m, \mu_m) = 0 \\ \sum_{j=1}^{8} \frac{\partial N_j}{\partial \mu}|_{(\xi_m,\eta_m,\mu_m)} \mathbf{X}_{m_j} \cdot \left( \mathbf{x}_s - \sum_{k=1}^{8} N_k|_{(\xi_m,\eta_m,\mu_m)} \cdot \mathbf{X}_{m_k} \right) \equiv f_2(\xi_m, \eta_m, \mu_m) = 0 \end{array} \right\} \tag{2.4}$$

The solution to (2.4) is obtained iteratively for the $(k+1)^{th}$ iteration as

$$\left\{ \begin{array}{c} \xi_m \\ \eta_m \\ \mu_m \end{array} \right\}^{k+1} = \left\{ \begin{array}{c} \xi_m \\ \eta_m \\ \mu_m \end{array} \right\}^{k} - \left[ \begin{array}{ccc} \frac{\partial f_1}{\partial \xi} & \frac{\partial f_1}{\partial \eta} & \frac{\partial f_1}{\partial \mu} \\ \frac{\partial f_2}{\partial \xi} & \frac{\partial f_2}{\partial \eta} & \frac{\partial f_2}{\partial \mu} \\ \frac{\partial f_3}{\partial \xi} & \frac{\partial f_3}{\partial \eta} & \frac{\partial f_3}{\partial \mu} \end{array} \right]^{-1} \left\{ \begin{array}{c} f_1 \\ f_2 \\ f_3 \end{array} \right\}$$

with the initial guess as $\left\{ \begin{array}{c} \xi_m \\ \eta_m \\ \mu_m \end{array} \right\}^{0} = \left\{ \begin{array}{c} 0 \\ 0 \\ 0 \end{array} \right\}$ and the RHS being evaluated based on the values $\left\{ \begin{array}{c} \xi_m \\ \eta_m \\ \mu_m \end{array} \right\}^{k}$ obtained from the previous $k^{th}$ iteration. The stopping criterion is

$$\| \left\{ \begin{array}{c} \xi_m \\ \eta_m \\ \mu_m \end{array} \right\}^{k+1} - \left\{ \begin{array}{c} \xi_m \\ \eta_m \\ \mu_m \end{array} \right\}^{k} \| < TOL * \| \left\{ \begin{array}{c} \xi_m \\ \eta_m \\ \mu_m \end{array} \right\}^{k} \|$$

where $TOL$ is a pre-specified tolerance.

## 3. Variation of the functional

Let $\mathbf{U}$ be the vector of displacement degrees of freedom at the finite element nodes and let $\mathbf{P}$ represent the vector of nodal forces. Then the system of equations after the

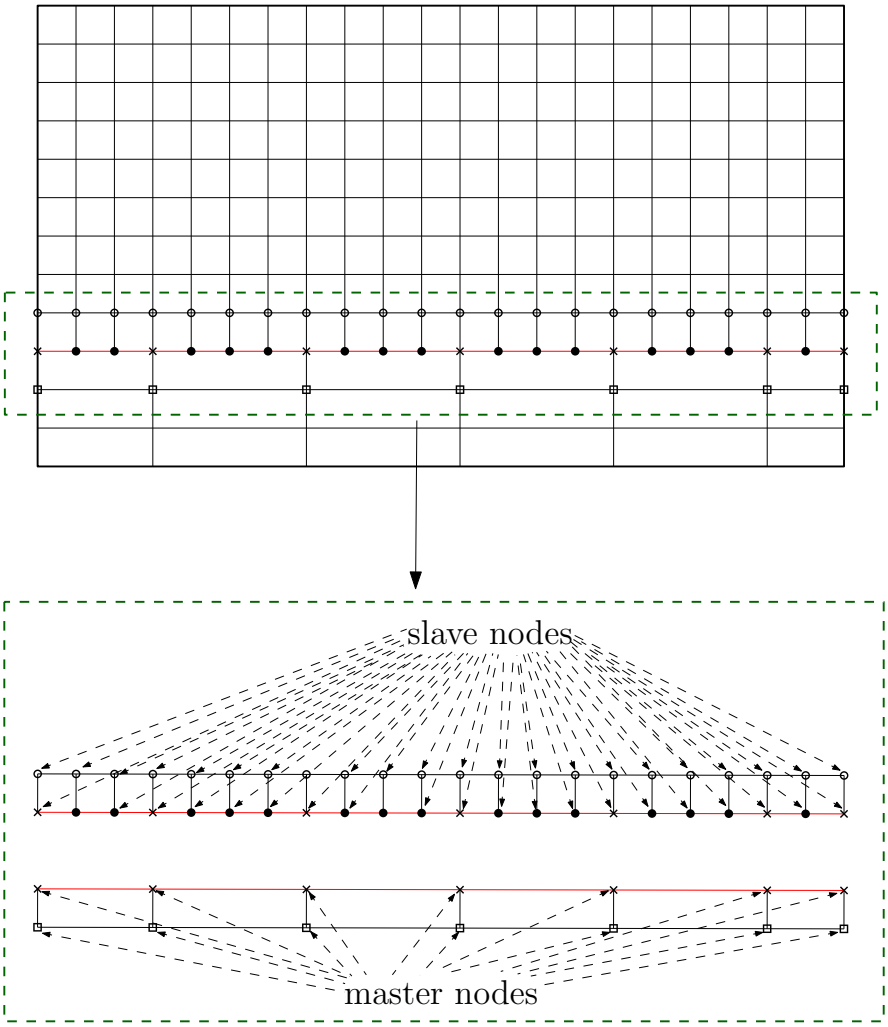


Figure 4: The lagrange multiplier term and penalty term are integrals with respect to the slave surface. 2D depiction for the sake of convenience

minimization of the augmented energy functional would be

$$\mathbf{KU} = \mathbf{P} \tag{3.1}$$

where $\mathbf{K}$ is the stiffness matrix. We rearrange the vector $\mathbf{U}$ in the following form

$$\mathbf{U} = \begin{Bmatrix} \mathbf{U}_r \\ \mathbf{U}_s \\ \mathbf{U}_m \end{Bmatrix}$$

where $\mathbf{U}_s$ are the displacement degrees of freedom corresponding to all the slave element nodes, $\mathbf{U}_m$ are the displacement degrees of freedom corresponding to all the master element

nodes and $\mathbf{U}_r$ are the displacement degrees of freedom corresponding to all the remaining nodes on the finite element mesh. The slave element nodes and master element nodes are identified in Figure 4. The system of equations (3.1) is then written as

$$\left[\mathbf{K}^d + \begin{bmatrix} . & . & . \\ . & \mathbf{K}_{ss} & \mathbf{K}_{sm} \\ . & \mathbf{K}_{ms} & \mathbf{K}_{mm} \end{bmatrix}\right] \begin{Bmatrix} \mathbf{U}_r \\ \mathbf{U}_s \\ \mathbf{U}_m \end{Bmatrix} = \mathbf{P} \tag{3.2}$$

where $\mathbf{K}^d$ is the stiffness matrix that is obtained after the minimization of the original energy functional. The objective is to obtain expressions for the submatrices $\mathbf{K}_{ss}$, $\mathbf{K}_{sm}$, $\mathbf{K}_{ms}$ and $\mathbf{K}_{mm}$ that arise as a result of the minimization of additional terms (lagrange multiplier term and penalty term) in the augmented energy functional. For the sake of clarity, we rewrite the augmented lagrangian functional as follows

$$\tilde{\mathscr{E}} \equiv \mathscr{E}^s + \mathscr{E}^m + \int_{\Gamma_c} \frac{1}{2}(\mathbf{t}^s + \mathbf{t}^m) \cdot \mathbf{g}\, dA + \frac{1}{2}\int_{\Gamma_c} \epsilon \mathbf{g} \cdot \mathbf{g}\, dA$$

The first variation of the energy functional would be

$$\delta\tilde{\mathscr{E}} = \delta(\mathscr{E}^s + \mathscr{E}^m) + \underbrace{\int_{\Gamma_c} \frac{1}{2}(\delta\mathbf{t}^s + \delta\mathbf{t}^m) \cdot \mathbf{g}\, dA + \int_{\Gamma_c} \frac{1}{2}(\mathbf{t}^s + \mathbf{t}^m) \cdot \delta\mathbf{g}\, dA + \int_{\Gamma_c} \epsilon \mathbf{g} \cdot \delta\mathbf{g}\, dA}_{\mathcal{C}}$$

which can also be written as

$$\delta\tilde{\mathscr{E}} = \delta\mathbf{U}^T(\mathbf{K}^d\mathbf{U} - \mathbf{P}) + \underbrace{\int_{\Gamma_c} \frac{1}{2}(\delta\mathbf{t}^s + \delta\mathbf{t}^m) \cdot \mathbf{g}\, dA + \int_{\Gamma_c} \frac{1}{2}(\mathbf{t}^s + \mathbf{t}^m) \cdot \delta\mathbf{g}\, dA + \int_{\Gamma_c} \epsilon \mathbf{g} \cdot \delta\mathbf{g}\, dA}_{\mathcal{C}} \tag{3.3}$$

## 4. Numerical integration for evaluation of surface integrals

The integral $\mathcal{C}$ in Equation (3.3) is evaluated as a sum of the integrands evaluated at the four gauss points multiplied by the determinant of the jacobian of the mapping from the reference 2D element to the slave surface as follows

$$\mathcal{C} = \sum_{N=1}^{4} \left[\frac{1}{2}(\delta\mathbf{t}^s + \delta\mathbf{t}^m) \cdot \mathbf{g} + \frac{1}{2}(\mathbf{t}^s + \mathbf{t}^m) \cdot \delta\mathbf{g} + \epsilon \mathbf{g} \cdot \delta\mathbf{g}\right] detJ \tag{4.1}$$

Now, corresponding to each gauss point on the reference element to which the slave surface is mapped onto, there is an orthogonal projection onto the master surface. We employ the logic elucidated in module 2.1 to evaluate those orthogonal projections.

*4.1. Evaluating the force conjugates one gauss point at a time*

The force conjugate to the constraint evaluated at $(\xi_s, \eta_s, \mu_s)$ is given by

$$\begin{aligned}
\mathbf{t}^s &= \begin{bmatrix} \sigma_1 & \sigma_4 & \sigma_6 \\ \sigma_4 & \sigma_2 & \sigma_5 \\ \sigma_6 & \sigma_5 & \sigma_3 \end{bmatrix} \Bigg|_{(\xi_s,\eta_s,\mu_s)} \begin{Bmatrix} n_1 \\ n_2 \\ n_3 \end{Bmatrix} \Bigg|_{(\xi_s,\eta_s,\mu_s)} \\
&\equiv \overbrace{\begin{bmatrix} n_1 & 0 & 0 & n_2 & 0 & n_3 \\ 0 & n_2 & 0 & n_1 & n_3 & 0 \\ 0 & 0 & n_3 & 0 & n_2 & n_1 \end{bmatrix}}^{\mathcal{N}} \Bigg|_{(\xi_s,\eta_s,\mu_s)} \begin{Bmatrix} \sigma_1 \\ \sigma_2 \\ \sigma_3 \\ \sigma_4 \\ \sigma_5 \\ \sigma_6 \end{Bmatrix} \Bigg|_{(\xi_s,\eta_s,\mu_s)} \\
&\equiv \overbrace{\mathcal{N}|_{(\xi_s,\eta_s,\mu_s)} \mathcal{D} \mathbf{B}|_{(\xi_s,\eta_s,\mu_s)}}^{\mathcal{F}_1} \mathbf{U}_s
\end{aligned} \tag{4.2}$$

where $\begin{Bmatrix} n_1 \\ n_2 \\ n_3 \end{Bmatrix} \Big|_{(\xi_s,\eta_s,\mu_s)}$ is the normal to the slave surface evaluated at $(\xi_s, \eta_s, \mu_s)$, $\mathcal{D}$ is the $6 \times 6$ constitutive matrix and $\mathbf{B}|_{(\xi_s,\eta_s,\mu_s)}$ is the $6 \times 24$ strain displacement interpolation matrix evaluated at $(\xi_s, \eta_s, \mu_s)$. Similarly, the force conjugate to the constraint evaluated at $(\xi_m, \eta_m, \mu_m)$ is given by

$$\mathbf{t}^m \equiv \overbrace{\mathcal{N}|_{(\xi_m,\eta_m,\mu_m)} \mathcal{D} \mathbf{B}|_{(\xi_m,\eta_m,\mu_m)}}^{\mathcal{F}_2} \mathbf{U}_m \tag{4.3}$$

where $\begin{Bmatrix} n_1 \\ n_2 \\ n_3 \end{Bmatrix} \Big|_{(\xi_m,\eta_m,\mu_m)}$ is the normal to the master surface evaluated at $(\xi_m, \eta_m, \mu_m)$ and $\mathbf{B}|_{(\xi_m,\eta_m,\mu_m)}$ is the $6 \times 24$ strain displacement interpolation matrix evaluated at $(\xi_m, \eta_m, \mu_m)$.

The normals $\left\{ \begin{array}{c} n_1 \\ n_2 \\ n_3 \end{array} \right\}\Big|_{(\xi_s,\eta_s,\mu_s)}$ and $\left\{ \begin{array}{c} n_1 \\ n_2 \\ n_3 \end{array} \right\}\Big|_{(\xi_m,\eta_m,\mu_m)}$ are obtained as follows

$$\left\{ \begin{array}{c} n_1 \\ n_2 \\ n_3 \end{array} \right\}\Big|_{(\xi_s,\eta_s,\mu_s)} = \frac{\nabla S_s}{\|\nabla S_s\|}\Big|_{(\xi_s,\eta_s,\mu_s)}$$

$$\left\{ \begin{array}{c} n_1 \\ n_2 \\ n_3 \end{array} \right\}\Big|_{(\xi_m,\eta_m,\mu_m)} = \frac{\nabla S_m}{\|\nabla S_m\|}\Big|_{(\xi_m,\eta_m,\mu_m)}$$

where $S_s$ and $S_m$ are equations of the slave and master surfaces respectively. The equations of the surfaces given coordinates of the four points are obtained using the procedure of singular value decompositions as described in Dana et al. [2].

*4.2. Evaluating the penetration function one gauss point at a time*

The penetration function is given by

$$\mathbf{g} = \mathbf{u}_s - \mathbf{u}_m = \overbrace{\mathbf{N}|_{(\xi_s,\eta_s,\mu_s)}}^{\mathcal{F}_3}\mathbf{U}_s - \overbrace{\mathbf{N}|_{(\xi_m,\eta_m,\mu_m)}}^{\mathcal{F}_4}\mathbf{U}_m \tag{4.4}$$

where $\mathbf{N}$ is the $3 \times 24$ shape function matrix

*4.3. Evaluating the surface integral*

In lieu of Equations (4.2) - (4.4), the surface integral (4.1) is evaluated as

$$\begin{aligned} \mathcal{C} = \sum_{N=1}^{4} \Bigg[ & \frac{1}{2}(\mathcal{F}_1\delta\mathbf{U}_s + \mathcal{F}_2\delta\mathbf{U}_m)\cdot(\mathcal{F}_3\mathbf{U}_s - \mathcal{F}_4\mathbf{U}_m) \\ & + \frac{1}{2}(\mathcal{F}_1\mathbf{U}_s + \mathcal{F}_2\mathbf{U}_m)\cdot(\mathcal{F}_3\delta\mathbf{U}_s - \mathcal{F}_4\delta\mathbf{U}_m) \\ & + \epsilon(\mathcal{F}_3\mathbf{U}_s - \mathcal{F}_4\mathbf{U}_m)\cdot(\mathcal{F}_3\delta\mathbf{U}_s - \mathcal{F}_4\delta\mathbf{U}_m) \Bigg] detJ \end{aligned}$$

which can also be written as

$$\mathcal{C} = \delta\mathbf{U}_s^T \underbrace{\left[ \sum_{N=1}^{4} \left[ \frac{1}{2}\mathcal{F}_1^T\mathcal{F}_3 + \frac{1}{2}\mathcal{F}_3^T\mathcal{F}_1 + \epsilon\mathcal{F}_3^T\mathcal{F}_3 \right] detJ \right]}_{\mathbf{K}_{ss}} \mathbf{U}_s$$

$$
\begin{aligned}
&+ \delta \mathbf{U}_s^T \underbrace{\left[ \sum_{N=1}^{4} \left[ -\frac{1}{2}\mathcal{F}_1^T \mathcal{F}_4 + \frac{1}{2}\mathcal{F}_3^T \mathcal{F}_2 - \epsilon \mathcal{F}_3^T \mathcal{F}_4 \right] detJ \right]}_{\mathbf{K}_{sm}} \mathbf{U}_m \\
&+ \delta \mathbf{U}_m^T \underbrace{\left[ \sum_{N=1}^{4} \left[ \frac{1}{2}\mathcal{F}_2^T \mathcal{F}_3 - \frac{1}{2}\mathcal{F}_4^T \mathcal{F}_1 - \epsilon \mathcal{F}_4^T \mathcal{F}_3 \right] detJ \right]}_{\mathbf{K}_{ms}} \mathbf{U}_s \\
&+ \delta \mathbf{U}_m^T \underbrace{\left[ \sum_{N=1}^{4} \left[ -\frac{1}{2}\mathcal{F}_2^T \mathcal{F}_4 - \frac{1}{2}\mathcal{F}_4^T \mathcal{F}_2 + \epsilon \mathcal{F}_4^T \mathcal{F}_4 \right] detJ \right]}_{\mathbf{K}_{mm}} \mathbf{U}_m
\end{aligned} \tag{4.5}
$$

## 5. System of Equations

The system of equations is obtained by equating the variation of the functional to zero as follows

$$\delta\tilde{\mathscr{C}} \equiv \delta \mathbf{U}^T (\mathbf{K}^d \mathbf{U} - \mathbf{P}) + \delta {\mathbf{U}_\mathbf{s}}^T \mathbf{K}_{ss} \mathbf{U}_s + \delta {\mathbf{U}_\mathbf{s}}^T \mathbf{K}_{sm} \mathbf{U}_m + \delta {\mathbf{U}_\mathbf{m}}^T \mathbf{K}_{ms} \mathbf{U}_s + \delta {\mathbf{U}_\mathbf{m}}^T \mathbf{K}_{mm} \mathbf{U}_m = 0$$

which is eventually written as

$$\left[ \mathbf{K}^d + \begin{bmatrix} . & . & . \\ . & \mathbf{K}_{ss} & \mathbf{K}_{sm} \\ . & \mathbf{K}_{ms} & \mathbf{K}_{mm} \end{bmatrix} \right] \begin{Bmatrix} \mathbf{U}_r \\ \mathbf{U}_s \\ \mathbf{U}_m \end{Bmatrix} = \mathbf{P}$$

where $\mathbf{K}_{ss}$, $\mathbf{K}_{sm}$, $\mathbf{K}_{ms}$ and $\mathbf{K}_{mm}$ are given in Equation (4.5).

## References


[1] R. Becker, P. Hansbo, and R. Stenberg. A finite element method for domain decomposition with non-matching grids. *ESAIM Mathematical Modelling and Numerical Analysis*, 37(2):209–225, 2003.

[2] S. Dana, B. Ganis, and M. F. Wheeler. A multiscale fixed stress split iterative scheme for coupled flow and poromechanics in deep subsurface reservoirs. *Journal of Computational Physics*, 352:1–22, 2018.

[3] N. El-Abbasi and K. J. Bathe. Stability and patch test performance of contact discretizations and a new solution algorithm. *Computers and Structures*, 79(16):1473–1486, 2001.

[4] C. A. Felippa. Iterative procedures for improving penalty function solutions of algebraic systems. *International Journal for Numerical Methods in Engineering*, 12(5):821–836, 1978.

[5] J. O. Hallquist, G. L. Goudreau, and D. J. Benson. Sliding interfaces with contact-impact in large-scale lagrangian computations. *Computer Methods in Applied Mechanics and Engineering*, 51:107–137, 1985.

[6] T. W. McDevitt and T. A. Laursen. A mortar-finite element formulation for frictional contact problems. *International Journal for Numerical Methods in Engineering*, 48 (10):1525–1547, 2000.

[7] P. Papadopoulos and R. L. Taylor. A mixed formulation for the finite element solution of contact problems. *Computer Methods in Applied Mechanics and Engineering*, 94(3): 373–389, 1992.

[8] P. Papadopoulos and R. L. Taylor. A simple algorithm for three-dimensional finite element analysis of contact problems. *Computers and Structures*, 46(6):1107–1118, 1993.

[9] H. Parisch. A consistent tangent stiffness matrix for three-dimensional non-linear contact analysis. *International Journal for Numerical Methods in Engineering*, 28(8): 1803–1812, 1989.

[10] M. J. D. Powell. Algorithms for nonlinear constraints that use lagrangian functions. *Mathematical Programming*, 14(1):224–248, 1978.

[11] M. A. Puso and T. A. Laursen. Mesh tying on curved interfaces in 3d. *Engineering Computations*, 20(3):305–319, 2003.

[12] M. A. Puso and T. A. Laursen. A mortar segment-to-segment contact method for large deformation solid mechanics. *Computer Methods in Applied Mechanics and Engineering*, 193(6-8):601–629, 2004.

[13] J. C. Simo, P. Wriggers, and R. L. Taylor. A perturbed lagrangian formulation for the

finite element solution of contact problems. *Computer Methods in Applied Mechanics and Engineering*, 50(2):163–180, 1985.

[14] P. Wriggers. *Computational Contact Mechanics*. Springer, 2nd edition, 2006.

[15] P. Wriggers and J. C. Simo. A note on tangent stiffness for fully nonlinear contact problems. *International Journal for Numerical Methods in Biomedical Engineering*, 1 (5):199–203, 1985.

[16] P. Wriggers and G. Zavarise. A formulation for frictionless contact problems using a weak form introduced by nitsche. *Computational Mechanics*, 41(3):407–420, 2008.